

# Chemical nanofabrication: a general route to surface-patterned and free-standing transition metal chalcogenide nanostructures†

Christopher L. Stender and Teri W. Odom\*

Received 5th December 2006, Accepted 10th January 2007

First published as an Advance Article on the web 16th January 2007

DOI: 10.1039/b617714j

This communication describes how chemical nanofabrication—a combination of bottom-up chemical methods and top-down nanoscale patterning—provides an approach to generate patterned and free-standing transition metal chalcogenide nanostructures.

Transition metal chalcogenide (TMC) materials are important in a range of applications from solar cells<sup>1</sup> to low friction surfaces<sup>2</sup> to battery electrode materials.<sup>3</sup> The ability to generate nanoscale structures of TMC materials offers new opportunities to optimize and improve their properties and to extend their usefulness. For example, fullerene-like TMCs (*e.g.* WS<sub>2</sub>, MoS<sub>2</sub> and TiS<sub>2</sub>) intercalated with Li exhibit greater loading capacity and are less air sensitive compared to bulk crystals; such properties are important for battery storage capacity.<sup>4</sup> WS<sub>2</sub> nanotubes exhibit a red shift in their band gap as the diameter of the tube decreases because of the increased elastic strain imposed on the molecular sheets,<sup>4</sup> and their high aspect ratios have made them useful as tips for scanning probe microscopies.<sup>5</sup> WS<sub>2</sub> and MoS<sub>2</sub> nanostructures have also demonstrated potential as additives to conventional lubricants by improving their general wear characteristics.<sup>6</sup>

Similar to synthetic approaches, chemical nanofabrication—the combination of nanoscale patterning and chemical methods<sup>7</sup>—can also create new types of functional nanostructures with unexpected properties. Nanoscale solid state ionic conducting materials, such as Ag<sub>2</sub>S, have been used as a basis for quantized controlled switching and have achieved faster switching speeds as a function of size.<sup>8</sup> Ribbons (5–50 μm wide) of Si and GaAs with thicknesses between 20–300 nm can be repeatedly stretched and compressed with no loss of structural or electronic integrity and have potential for use in flexible electronics.<sup>9,10</sup> Nanoscale wells with zL volumes in silicon substrates have functioned as nanoscale beakers to grow crystalline CdS nanoparticles at room temperature.<sup>11</sup> Single crystalline nanowires of Ag<sub>2</sub>Se and CdSe have also been synthesized by a low temperature chemical transformation of pre-formed Se nanowires.<sup>12</sup> In addition, we have found that a reduction in the size of Mo metal nanopatterns prior to their chemical conversion in H<sub>2</sub>S gas resulted in the preferential orientation of MoS<sub>2</sub> nanocrystals within patterned MoS<sub>2</sub> structures.<sup>13</sup>

This paper reports how chemical nanofabrication can be used to generate patterned and free-standing TMC nanostructures out of different metals and different chalcogens. We demonstrate the generality and flexibility of this approach by (1) patterning arrays

of M<sub>n</sub>X<sub>y</sub> (M = Ni, Ag; X = S, Se) nanoscale structures with different shapes and sizes; (2) fabricating crossed arrays of nanostructures out of different TMC materials using a two-stage conversion process; and (3) creating free-standing nanostructures of NiS<sub>2</sub> materials. We can control independently the width, height and aspect ratio of the TMC structures as well as the pitch and area (>1 in<sup>2</sup>) over which they are patterned.

Fig. 1(a) outlines our procedure to pattern TMC structures composed of nanoscale crystals. We have illustrated this general approach by focusing on a specific metal, nickel, patterned on a Si substrate. First, phase shifting photolithography (PSP) with a *h*-PDMS mask patterned with recessed 3 μm circles was used to generate rings with sub-200 nm trenches in a negative-tone photoresist (*ma N-405*) (Fig. 1(b)).<sup>14</sup> We then deposited by e-beam evaporation a thin (~2 nm) adhesion layer of Ti followed by 70 nm of Ni to produce Ni rings after lift-off of the photoresist

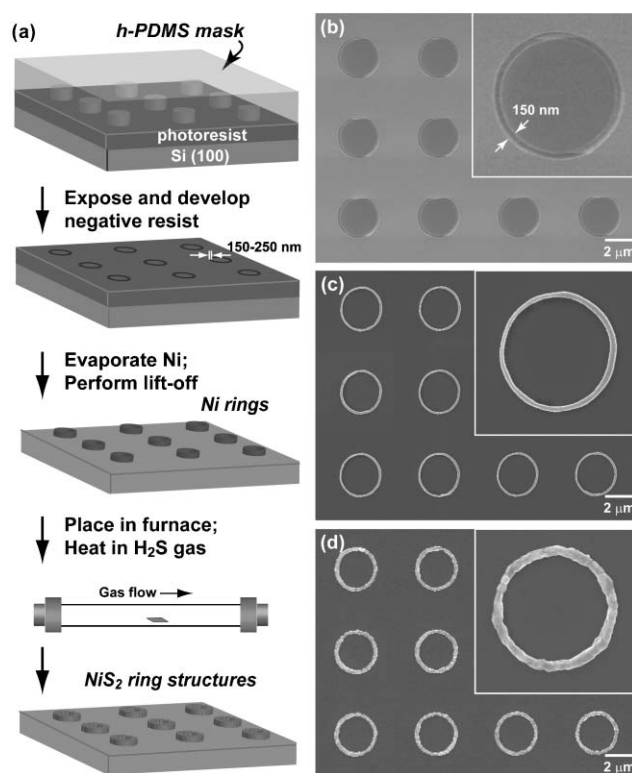


**Fig. 1** (a) Schematic outline of the procedure to generate arrays of TMCs. (b) Scanning electron microscopy (SEM) image of an array of recessed rings in negative-tone photoresist. (c) SEM image of an array of Ni rings. (d) SEM image of an array of NiS<sub>2</sub> rings after chemical conversion of Ni rings in (b). All insets are 4 μm × 4 μm.

Department of Chemistry, Northwestern University, 2145 Sheridan Road, Evanston, IL 60208, USA. E-mail: todom@northwestern.edu  
† This paper is part of a *Journal of Materials Chemistry* issue highlighting the work of emerging investigators in materials chemistry.

(Fig. 1(c)). To convert the metal to its metal sulfide, we placed the nanopatterned Ni sample into a 1 in quartz tube furnace for 10 h at 400 °C (2 °C min<sup>-1</sup>) under a flow of argon ( $P_{Ar} \sim 646$  Torr) and H<sub>2</sub>S ( $P_{H_2S} \sim 114$  Torr) gases. The Ni rings were converted to NiS<sub>2</sub> ring structures, whose widths were 260–290 nm and heights were 115–140 nm (Fig. 1(d)).

Surprisingly, the NiS<sub>2</sub> structures were composed of nanocrystals that overlapped with each other to form a continuous network (Fig. 2). The edges of the crystals followed the direction of the patterned metal structures, both for curved (Fig. 2(a), insets) and straight patterns (Fig. 2(b)). Fig. 2(b) shows one dimensional arrays of NiS<sub>2</sub> lines that are spaced by 400 nm. Although the crystals in these lines were also connected, on careful inspection, it was obvious that individual lines were not identical; the crystal facets had slightly different orientations along the patterned lines. To determine the crystal structure of the patterned NiS<sub>2</sub> materials, we used glancing angle X-ray diffraction (GAXD). This technique allowed us to characterize the crystal structure of relatively low density nanostructures, and at the same time, preserve their integrity on a surface. GAXD spectra were consistent with bulk cubic NiS<sub>2</sub> (PDF #01-089-3058, space group  $Pa\bar{3}$ ) (Fig. 2(c)). In some cases, the X-ray angle of incidence was not steep enough, and we occasionally picked up peaks from the underlying Si substrate.

In contrast to our previous work on MoS<sub>2</sub> nanostructures,<sup>13</sup> the crystals in the NiS<sub>2</sub> structures did not exhibit preferential orientation depending on their location within the tube furnace. It is possible that this difference is because of the different crystal structures, since synthetic MoS<sub>2</sub> is a layered material with Mo atoms trigonally coordinated to S atoms in a sandwich arrangement with three layers per unit, while NiS<sub>2</sub> is cubic with Ni atoms coordinated to six S atoms in a pyrite lattice structure. Also, the crystals comprising the MoS<sub>2</sub> structures were more discrete, while for NiS<sub>2</sub>, the overlapping nanocrystals formed continuous structures.

Our chemical nanofabrication approach to TMC nanomaterials can be readily extended to form metal selenide nanostructures. Instead of reaction of the patterned metal nanostructures in the tube furnace with H<sub>2</sub>S gas, we can expose them to Se vapor formed by sublimation of solid Se powder. This quasi-solid state reaction with solid Se has been used by others to synthesize one dimensional nanostructures.<sup>15</sup> After carrying out PSP with *h*-PDMS masks patterned with 2 μm lines spaced by 2 μm on negative photoresist, we deposited 60 nm of Ag and performed lift-off to generate lines of Ag. We then placed this substrate into the tube furnace with Se powder. The chamber was purged several times with argon gas and evacuated to ~8 mTorr and held at 200 °C for 20 min. Fig. 3(a) depicts lines of Ag<sub>2</sub>Se that were formed after reacting the Ag lines with Se. Noticeably, the structures do not exhibit well-formed facets like the NiS<sub>2</sub> structures. The GAXD spectrum revealed, however, that the Ag<sub>2</sub>Se structures were orthorhombic (PDF #01-089-2591, space group  $P2221$ ) (Fig. 3(b)).

Because we use soft masks for photolithography, we can perform multiple patterning steps to create arrays of structures of different TMC materials on the same substrate. We have developed a two-stage conversion process to fabricate crossed arrays of different materials. This procedure can be summarized by four steps: (1) nanopatterning the first metal (M1) using PSP

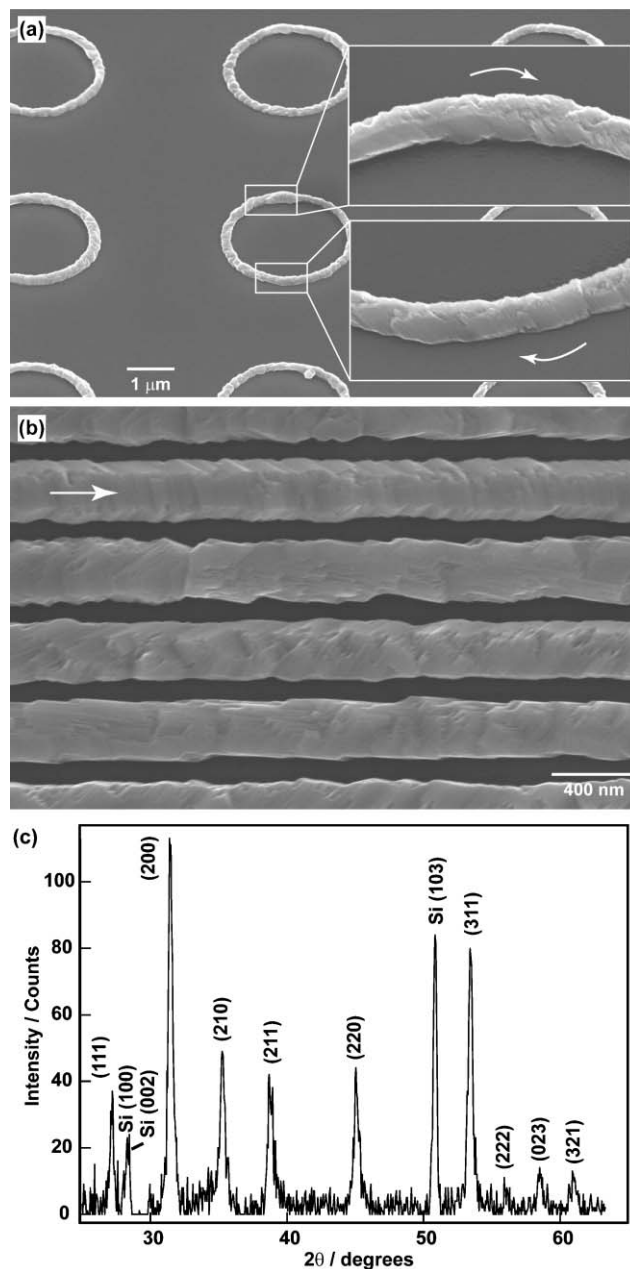


**Fig. 2** (a) SEM image of arrays of NiS<sub>2</sub> rings. The tilt angle is 45°. The insets depict how the nanocrystals within the NiS<sub>2</sub> ring overlap with each other and follow the curved direction of the pattern. (b) SEM image of NiS<sub>2</sub> lines generated on a 400 nm pitch. Each line is a continuous structure although the nanocrystal facets are oriented at slightly different angles along the line. (c) Glancing angle X-ray diffraction (GAXD) spectrum of nanopatterned NiS<sub>2</sub> lines exhibiting characteristic peaks for cubic NiS<sub>2</sub> (PDF #01-089-3058).

followed by deposition and lift-off; (2) converting M1 to its sulfide analog; (3) nanopatterning the second metal (M2) using PSP followed by deposition and lift-off; and (4) converting M2 to its selenide counterpart.

We have carried out this procedure by first generating 250 nm lines of NiS<sub>2</sub> on a 2 μm pitch. Then, we spin-cast negative-tone photoresist (*ma* N-405) over the NiS<sub>2</sub> pattern and performed PSP with masks patterned with microscale lines having variable pitch

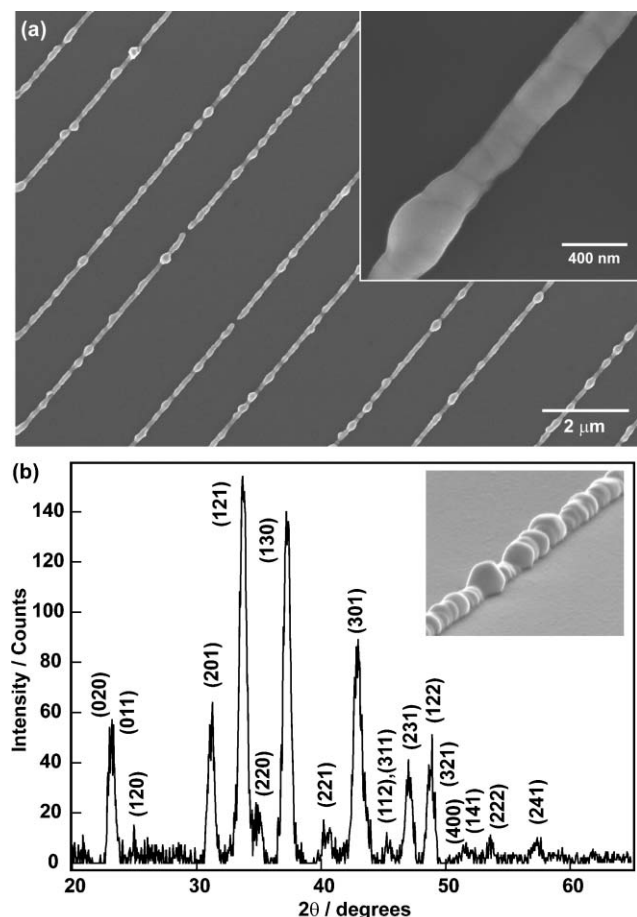


**Fig. 3** (a) SEM image of Ag lines converted to  $\text{Ag}_2\text{Se}$  using quasi-solid state reaction conditions. Inset shows a zoom-in of one of the  $\text{Ag}_2\text{Se}$  lines. (b) GAXD spectrum of lines in (a) exhibiting characteristic peaks for orthorhombic  $\text{Ag}_2\text{Se}$  (PDF #01-089-2591).

and oriented perpendicular to the  $\text{NiS}_2$  lines. Even after evaporation of 60 nm of Ag followed by lift-off of the photoresist, the  $\text{NiS}_2$  structures were robust and stayed intact, which provides additional evidence that the structures were continuous. This secondary patterning could not be achieved using standard Cr masks in contact photolithography because the hard contact would damage the substrates. We then placed the  $\text{NiS}_2/\text{Ag}$  crossed arrays into a quartz tube furnace along with Se powder source material and evacuated and heated the chamber to 200 °C. Fig. 4 shows arrays of lines of  $\text{NiS}_2$  crossed by lines of  $\text{Ag}_2\text{Se}$ , which appear to be continuous across the intersection. The lines in the array can also be on any pitch because they are determined by the PDMS mask. We have demonstrated this versatility by patterning the  $\text{Ag}_2\text{Se}$  lines on a 2  $\mu\text{m}$  (Fig. 4(a)) and 10  $\mu\text{m}$  (Fig. 4(b)) pitch. Electron dispersive X-ray (EDX) analysis (not shown) indicated that each line was composed of the intended elements and that very little Se was incorporated into the  $\text{NiS}_2$  structures under these conditions.

Because the  $\text{NiS}_2$  nanomaterials are continuous, it should be possible to release them from the surface to form free-standing TMC structures. For this case, we modified our nanopatterning method but kept the chemical conversion conditions the same. Fig. 5(a) outlines the procedure for creating free-standing  $\text{NiS}_2$

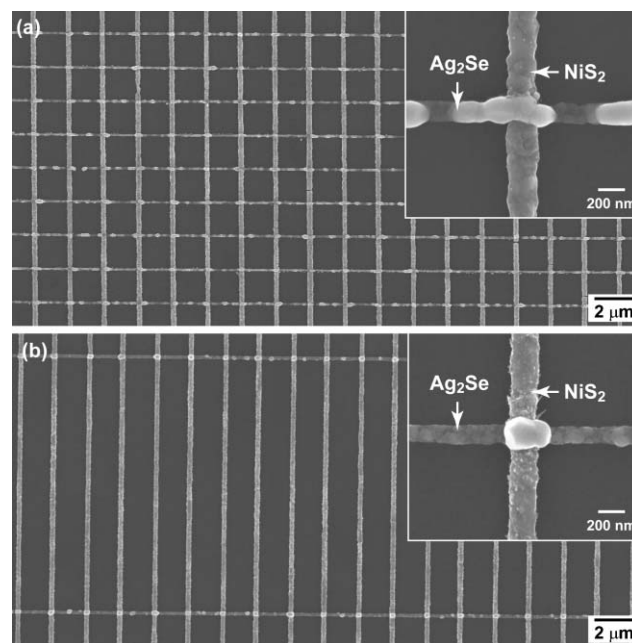


**Fig. 4** (a) SEM image of lines of  $\text{NiS}_2$  crossed by lines of  $\text{Ag}_2\text{Se}$  generated in a two-step process as described in the text. The  $\text{Ag}_2\text{Se}$  lines are spaced by 2  $\mu\text{m}$ . The inset shows that the  $\text{Ag}_2\text{Se}$  lines remain continuous over the underlying  $\text{NiS}_2$  lines. (b) SEM image of lines of  $\text{NiS}_2$  crossed by lines of  $\text{Ag}_2\text{Se}$  where the  $\text{Ag}_2\text{Se}$  lines are on 10  $\mu\text{m}$  pitch.

nanomaterials. First, we performed PSP using *h*-PDMS masks patterned with recessed parallelograms on positive-tone photoresist (Shipley 1805) to produce outlines of the parallelograms supported on Si (100) substrates.<sup>16</sup> We then deposited a thin (30 nm) layer of Cr and performed lift-off to form a Cr film with slots exposing the underlying Si. The sample was placed in an anisotropic Si etch (isopropanol-KOH, 72 °C), where the exposed Si was etched to form recessed “V” grooves, whose facets were Si (111) planes. We then deposited 50 nm of Ni into the grooves and removed the Cr film by wet chemical etching to form Ni rings inside the Si grooves. These Ni ring patterns were then placed into the tube furnace and converted to  $\text{NiS}_2$  (Fig. 5(b)). These  $\text{NiS}_2$  structures supported by Si were subjected briefly (50–80 s) to an anisotropic Si etch to release the parallelograms (Fig. 5(c)–(e)). The free-standing structures can also be dispersed in solution or transferred to other substrates.

In summary, we have demonstrated how chemical nanofabrication provides a general method to produce patterned and free-standing TMC nanomaterials. We have used this bottom-up meets top-down strategy to generate arrays of continuous  $\text{NiS}_2$  and  $\text{Ag}_2\text{Se}$  structures with controlled shapes and sizes, crossed line arrays of  $\text{NiS}_2/\text{Ag}_2\text{Se}$ , and free-standing  $\text{NiS}_2$  structures. These types of TMC nanostructures cannot easily be obtained by other chemical or fabrication-only methods. A limitation of our strategy for crossed arrays is that the metal sulfide nanopatterns must be stable in a Se-rich atmosphere (and at elevated temperature); any such reactivity could be useful, however, to create patterned solid solutions. Also, one drawback of our technique to generate free-standing structures is that the TMC should be compatible with KOH etch solutions; however, a dry Si etch in  $\text{XeF}_2$  can also release the TMC nanostructures. Our ability to generate

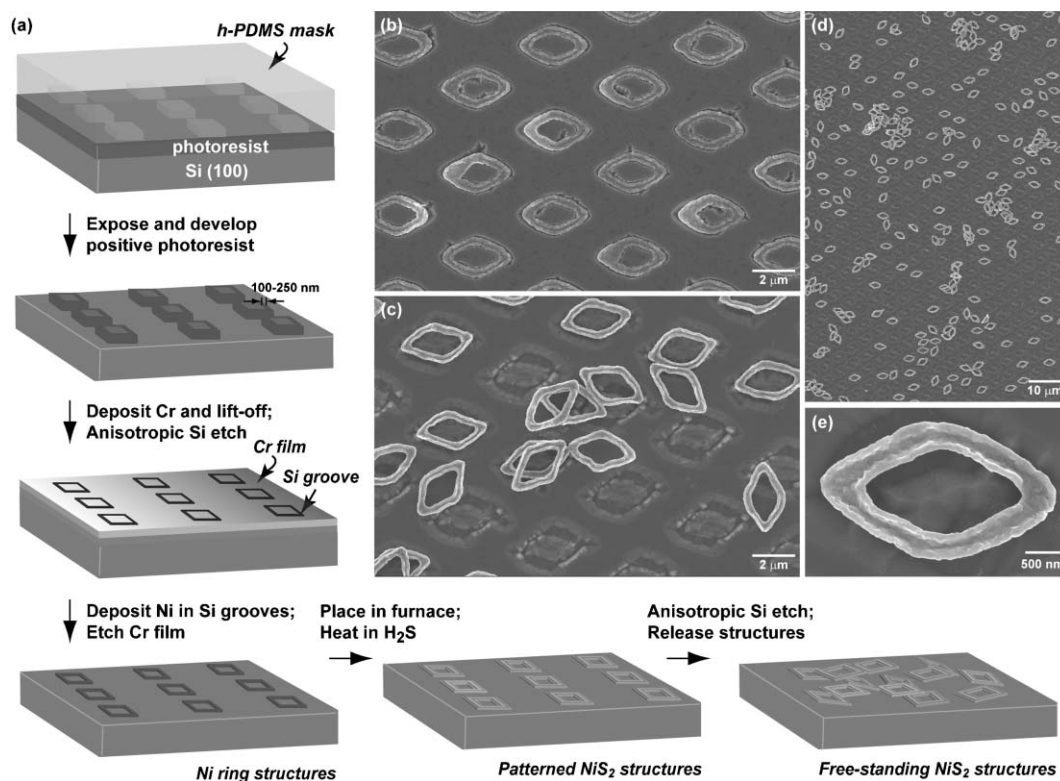


**Fig. 5** (a) Schematic outline of the procedure to generate free-standing NiS<sub>2</sub> structures. (b) SEM image of NiS<sub>2</sub> parallelograms within etched Si grooves. (c) SEM image of free-standing NiS<sub>2</sub> structures after they have been released from the substrate by a brief anisotropic Si etch. (d) Large-area image of free-standing NiS<sub>2</sub> parallelograms. (e) Zoom-in of an individual NiS<sub>2</sub> structure, which is robust and intact after removal from the template.

nanopatterned arrays of different TMCs, and in addition, free-standing TMC nanostructures, will certainly open new scientific prospects and contribute to emerging technologies based on TMCs.

## Acknowledgements

This research was supported by an NSF CAREER Award (CHE-0349302). This work made use of the NUANCE Center facilities and the J. B. Cohen X-Ray Diffraction Facility, which are supported by NSF-NSEC, NSF-MRSEC, and the Keck Foundation at Northwestern University. T.W.O. is a DuPont Young Professor, an Alfred P. Sloan Research Fellow, a Cottrell Scholar of Research Corporation, and a David and Lucile Packard Fellow.

## Notes and references

- 1 A. Olivas, J. Cruz-Reyes, V. Petranovskii, M. Avalos and S. Fuentes, *J. Vac. Sci. Technol., A*, 1998, **16**, 3515–3520.
- 2 I. L. Singer, S. Fayeulle and P. D. Ehni, *Wear*, 1996, **195**, 7–20.
- 3 I. Rom and W. Sitte, *Solid State Ionics*, 1997, **101–103**, 381–386.
- 4 R. Tenne, *J. Mater. Res.*, 2006, **21**, 2726–2743.
- 5 A. Rothschild, S. R. Cohen and R. Tenne, *Appl. Phys. Lett.*, 1999, **75**.
- 6 L. Rapoport, N. Fleischer and R. Tenne, *J. Mater. Chem.*, 2005, **15**, 1782–1788.
- 7 J. Henzie, J. E. Barton, C. L. Stender and T. W. Odom, *Acc. Chem. Res.*, 2006, **39**, 249–257.
- 8 K. Terabe, T. Hasagawa, T. Nakayama and M. Aono, *Nature*, 2005, **433**, 47–50.
- 9 D. Y. Khang, H. Jiang, Y. Huang and J. A. Rogers, *Science*, 2006, **311**, 208–212.
- 10 Y. Sun, H. Kim, E. Menard, S. Kim, I. Adesida and J. A. Rogers, *Small*, 2006, **11**, 1330–1334.
- 11 J. Barton and T. W. Odom, *Nano Lett.*, 2004, **4**, 1525–1528.
- 12 U. Jeong, P. H. C. Camargo, H. W. Lee and Y. Xia, *J. Mater. Chem.*, 2006, **16**, 3893–3897.
- 13 C. L. Stender, E. C. Greyson, Y. Babayan and T. W. Odom, *Adv. Mater.*, 2005, **17**, 2837–2481.
- 14 Y. Babayan, J. Barton, E. C. Greyson and T. W. Odom, *Adv. Mater.*, 2004, **16**, 1348–1352.
- 15 Y. S. Hor, Z. L. Xiao, U. Welp, Y. Ito, J. F. Mitchell, R. E. Cook, W. K. Kwok and G. W. Crabtree, *Nano Lett.*, 2005, **5**, 397–401.
- 16 T. W. Odom, J. C. Love, D. B. Wolfe, K. E. Paul and G. M. Whitesides, *Langmuir*, 2002, **18**, 5314–5320.